Journal of Peptide Science
J. Pept. Sci. 2008; **14**: 1195–1202
Published online 21 July 2008 in Wiley InterScience (www.interscience.wiley.com). DOI: 10.1002/psc.1060

JOURNAL OF PEPTIDE SCIENCE

Structure–activity relationships of α_{IIb} 313–320 derived peptide inhibitors of human platelet aggregation

RUXANDRA MARIA STANICA,[a] DIMITRA BENAKI,[b] FOTEINI I. RODIS,[a] EMMANUEL MIKROS,[c] DIMOKRITOS TSOUKATOS,[a] ALEXANDROS TSELEPIS[a] and VASILIOS TSIKARIS[a]*

[a] Department of Chemistry, University of Ioannina, 45110 Ioannina, Greece
[b] Institute of Biology, NCSR ''Demokritos'', 15310 Athens, Greece
[c] Department of Pharmacy, University of Athens, 15771 Athens, Greece

Received 6 March 2008; Revised 26 May 2008; Accepted 6 June 2008

Abstract: The $\alpha_{IIb}\beta_3$ receptor, which is the most abundant receptor on the surface of platelets, can interact with a variety of adhesive proteins including fibrinogen, fibronectin and the von Willebrand factor. Fibrinogen binding on $\alpha_{IIb}\beta_3$ is an event essential for platelet aggregation and thrombus formation. Mapping of the fibrinogen-binding domains on α_{IIb} subunit suggested the sequence 313–332 as a possible binding site. This region was restricted to sequence α_{IIb} 313–320 (Y^{313}MESRADR^{320}) using synthetic octapeptides overlapping by six residues. The YMESRADR octapeptide inhibits ADP-stimulated human platelets aggregation and binds to immobilized fibrinogen. In this study, we used the Ala scanning methodology within the sequence 313–320 aiming to evaluate the contribution of each amino acid in inhibiting platelet aggregation. It was found that the substitution of Y^{313}, M^{314}, E^{315} or S^{316} by A does not affect the activity of the parent octapeptide. The–RADR-motif seems to be the most essential for the biological activity of the α_{IIb} 313–320 site. The conformational analysis of the YAESRADR, YMESAADR and YMESRAAR analogs by using NMR spectroscopy and distance geometry calculations revealed significant differences in their conformational states in DMSO-d_6. Copyright © 2008 European Peptide Society and John Wiley & Sons, Ltd.

Keywords: α_{IIb} binding sites; arginine interactions; aspartic acid interactions; fibrinogen inhibitors; integrin $\alpha_{IIb}\beta_3$; NMR of peptides; RGD conformation; SARS

INTRODUCTION

The $\alpha_{IIb}\beta_3$ receptor, a member of the integrin family, plays an important role in human platelet aggregation. It interacts with a variety of adhesive proteins including fibrinogen, fibronectin and the von Willebrand factor [1,2]. The clarification of the mechanisms of $\alpha_{IIb}\beta_3$–fibrinogen interaction for understanding hemostasis and thrombosis, is an extremely contraversial issue. Blocking of fibrinogen–$\alpha_{IIb}\beta_3$ interaction due to quantitative and/or qualitative defects in platelet $\alpha_{IIb}\beta_3$ leads to a hemorrhagic disorder known as Glanzmann's thrombasthenia, while an excessive $\alpha_{IIb}\beta_3$–fibrinogen interaction could cause thrombosis [3]. The studies for determining the binding sites of $\alpha_{IIb}\beta_3$ started three decades ago. Combinations of immunological, biochemical, mutational approaches and peptide studies have been applied for mapping epitopes and identifying residues of $\alpha_{IIb}\beta_3$ implicated in ligand-binding function [4]. In a previous study, using synthetic 20 peptides derived from the sequence of the α_{IIb} subunit, and overlapped by 8 residues, we identified α_{IIb} 313–332 (Y^{313}MESRADRKLAEVGRVYLFL^{332}) region as a possible site involved in $\alpha_{IIb}\beta_3$–fibrinogen interaction [5]. The synthetic peptide α_{IIb} 313–332 inhibits platelet aggregation and fibrinogen binding to activated $\alpha_{IIb}\beta_3$. Interestingly, within the site α_{IIb} 313–332, two naturally occurring mutations (E324K and R327H) have been reported in patients with Glanzmann's thrombasthenia [6–9]. Moreover, it has been shown that the peptide LSARLAF binds to complementary region 315–321 of α_{IIb} and induces $\alpha_{IIb}\beta_3$ conformational change and platelet aggregation [10,11]. Binding of this peptide to α_{IIb} also induces platelet secretion and further activation through a $\alpha_{IIb}\beta_3$-mediated outside-in signal transduction [10–12].

In an attempt to restrict the active site α_{IIb} 313–332 we used synthetic octapeptide analogs derived from the entire sequence and overlapping by six residues. Seven octapeptides have been synthesized and tested for their ability to inhibit platelet aggregation and fibrinogen binding to activated $\alpha_{IIb}\beta_3$ receptor [13]. It was shown that the octapeptide Y^{313}MESRADR^{320} retains almost the same inhibitory activity as the α_{IIb} 313–332 sequence, which decreases in the cases of E^{315}SRADRKL^{322} and R^{317}ADRKLAE^{324} [13]. The common feature of the three peptides is the RAD sequence, which can be considered as an RGD analog. However, inhibition experiments performed in the presence of Pac-1, a monoclonal antibody which binds to activated $\alpha_{IIb}\beta_3$, have shown that PAC-1 binding to the receptor was not affected by any of those peptides, in contrast to RGDS positive control, which significantly inhibited PAC-1 binding [13]. This result suggests

*Correspondence to: Vasilios Tsikaris, Department of Chemistry, University of Ioannina, GR-45110 Ioannina, Greece;
e-mail: btsikari@cc.uoi.gr

that Y^{313}MESRADR^{320} inhibits fibrinogen binding to the activated receptor as well as platelet aggregation by a non-RGD-like mechanism. It seems that YMES sequence plays a key role in the activity and mode of action of Y^{313}MESRADR^{320} [13,14].

In this work, using Ala scanning methodology, we attempted to estimate the role of each amino acid within the α_{IIb} 313–320 sequence in inhibiting the platelet aggregation and to evaluate the structure–activity relationship. Eight octapeptides Y^{313}MESRADR^{320} (8pα_{IIb}313–320, control peptide), **A**^{313}MESRADR^{320} (8pα_{IIb}313A), Y^{313}**A**ESRADR^{320} (8pα_{IIb}314A), Y^{313}M**A**SRADR^{320} (8pα_{IIb}315A), Y^{313}ME**A**-RADR^{320} (8pα_{IIb}316A), Y^{313}MES**A**ADR^{320} (8pα_{IIb}317A), Y^{313}MESRA**A**R^{320} (8pα_{IIb}319A), Y^{313}MESRAD**A**^{320} (8p-α_{IIb}320A) were synthesized, and their effect on platelet aggregation was studied. Three analogs, 8pα_{IIb}314A (active), 8pα_{IIb}317A (inactive) and 8pα_{IIb}319A (inactive) were selected for conformational analysis by using NMR spectroscopy and distance geometry calculations. Considerable differences in their conformational states in DMSO-d_6 were shown to occur, which can be correlated with their inhibitory activity on platelet aggregation. Our results suggest that the R^{317} and D^{319} residues are required for retaining the inhibitory activity, and they strongly contribute to the stabilization of the conformation of the active analog Y^{313}AESRADR^{320}.

MATERIALS AND METHODS

Reagents

Abbreviations used in this paper follow the guidelines by Jones JH [15]. Fmoc amino acid derivatives, HBTU and HOBt were purchased from Neosystem Laboratoire (Strasbourg, France). 4-(Hydroxymethyl) phenoxymethyl-linked polystyrene (Wang) resins were obtained from GL Biochem (Shanghai, China). Triisopropylsilane (TIS), 1,2-ethane dithiol (EDT), diisopropylethylamine (DIEA), TFA, dimethoxybenzene (DMB), piperidine, were Merck-Schuchardt (Darmstadt, Germany) products and used without further purification. DCM, DMF distilled over ninhydrin and stored under preactivated molecular sieves 4 Å, and the gradient degree HPLC solvents acetonitrile and methanol were purchased from Labscan (Dublin, Ireland).

HPLC Analysis

The analytical HPLC chromatograms were run on a Waters Millenium (Milford, USA) apparatus with a photodiode array detector 996. The spectra were acquired at 214 and 280 nm. A reverse-phase Discovery C18 column and a flow rate of 1 ml/min were used. The crude peptides were purified by semipreparative HPLC on a Water PrepLC 4000 system associated with a reversed-phase Discovery C18 column (25 cm × 10 mm) running at a flow rate of 4.7 ml/min.

Electrospray Mass Spectroscopy

Electrospray mass spectra were recorded on a Micromass (Manchester, England) Platform II quadrupole mass spectrometer. Samples were dissolved in the mixture $H_2O/CH_3CN/HCOOH$ (49 : 49 : 2) and injected into the ESI source at a flow rate of 5 µl/min. The source temperature was adjusted at 60 °C, while the cone voltage was set to 60 V.

Peptides Synthesis

Seven peptides were synthesized on a Wang resin (0.75 meq g^{-1} resin) using the standard SPPS methodology [16–18]. The coupling of the first amino acid on the resin was performed by using an amino acid/HBTU/HOBt/DIEA/resin molar ratio 3 : 3 : 3 : 6 : 1 in a 20% 4-dimetylaminopyridine/DMF solution. Aspartic and glutamic acids were introduced as Fmoc-Asp-(O*t*Bu)-OH and Fmoc-Glu-(O*t*Bu)-OH, respectively, arginine as Fmoc-Arg-(Pbf)-OH, serine and tyrosine as Fmoc-Ser-(*t*Bu)-OH and Fmoc-Tyr-(*t*Bu)-OH. Fmoc protective groups were removed with 20% (v/v) piperidine in DMF. Couplings were performed by using an amino acid/HBTU/HOBt/DIEA/resin molar ratio 3 : 3 : 3 : 6 : 1. The crude peptides were obtained by treatment of the peptide–resin for 3 h with a mixture of TFA/TIS/H_2O (95 : 2.5 : 2.5, v/v/v). In the case of methionine-containing peptides the peptide–resin was treated for 3.5 h with a mixture TFA/TIS/EDT/H_2O (94 : 2.5 : 2.5 : 1, v/v/v/v). The resin was filtered and washed with TFA. The combined filtrates were concentrated under reduced pressure. Hexane was added and the mixture was reconcentrated. This procedure was performed twice. The peptides were precipitated with cold diethyl ether, filtered, dissolved in 2N acetic acid, and lyophilized (yields ranged from 85 to 95%). Peptides were purified by semipreparative reverse HPLC. Gradient elution was performed with the following solvents: A, H_2O/0.1% TFA, and B, CH_3CN/0.1% TFA, v/v). Yields at the purification step ranged from 45 to 65%. The purified peptides were analyzed by HPLC and ESI-MS (Table 1).

Platelet Aggregation Assays

Fresh platelet-rich plasma (PRP) was prepared from the whole blood of healthy volunteers by centrifugation at 160 *g* for 10 min at room temperature [13,14]. Blood was anticoagulated with an aqueous solution consisting of sodium citrate (2.2%), citrate acid (0.8%) and glucose (2.5%). The remaining blood specimen was centrifuged at 3000 *g* for 20 min to prepare platelet-poor plasma (PPP). Assessment of functional blockage of GPIIb/IIIa was made utilizing ADP-induced platelet aggregation in PRP, and it was determined by the measured change in light transmission (PPP represents 100%), through the PRP (2.5×10^5 platelet/ml), on a Chrono-Log Model 500-Ca Lumi-Aggregometer, under stirring conditions. The aggregation was initiated by adding 5 µM ADP; the peptide analogs were added 1 min later in tris-buffer saline (TBS) at pH 7.4, and the reaction was then allowed to proceed for further 3 min. The inhibitory activity of the peptides in the ADP-induced platelets aggregation was measured. The results were expressed as mean ± SD. Mean values were compared by Student's *t*-test, with significance defined at a value of $P < 0.05$.

^{1}H-NMR Experiments

The NMR samples were prepared by dissolving the solid peptide in H_2O and adjusting the pH to the desired value

DOI: 10.1002/psc

Table 1 ESI-MS, HPLC and inhibitory activity data of the studied peptides

Analog	Sequence	M.W. calc./found	HPLC retention time (min)[a]	Inhibition of platelet aggregation (%)[b]
8pα_{IIb}313–320 control peptide	Y^{313}MESRADR^{320}	1027.13/1027.17	8.6	56 ± 9
8pα_{IIb}313A	**A**^{313}MESRADR^{320}	935.03/935.27	7.4	59 ± 4
8pα_{IIb}314A	Y^{313}**A**ESRADR^{320}	967.01/967.10	8.2	57 ± 10
8pα_{IIb}315A	Y^{313}M**A**SRADR^{320}	969.09/969.27	9.9	56 ± 12
8pα_{IIb}316A	Y^{313}ME**A**RADR^{320}	1011.13/1011.39	9.5	52 ± 5
8pα_{IIb}317A	Y^{313}MES**A**ADR^{320}	942.02/941.85	9.8	28 ± 6*
8pα_{IIb}319A	Y^{313}MESRA**A**R^{320}	983.12/982.89	9.6	9 ± 1**
8pα_{IIb}320A	Y^{313}MESRAD**A**^{320}	942.02/942.11	9.9	53 ± 4

[a] For details see Material and Methods.
[b] Values are the mean ± SD from eight different platelet preparations and represent the inhibitory effect of each peptide at a concentration of 500 μM on platelet aggregation induced by 5 μM ADP. Statistical analysis was performed by unpaired Student's *t*-test, and differences were considered significant at $P < 0.05$. * $P < 0.03$ and ** $P < 0.01$ compared to 8pα_{IIb}313A, 8pα_{IIb}314A, 8pα_{IIb}315A, 8pα_{IIb}316A and 8pα_{IIb}320A.

with NaOH or HCl. The aqueous solutions were lyophilized, and weighted amounts were dissolved in DMSO-d_6 at concentrations ~5–8 mM [19]. The NMR experiments were performed at 300–340 K on a Bruker Avance DRX-400 MHz spectrometer, with the probe temperature maintained using a BVT-3000 Bruker control unit. 1D spectra were acquired using 16 K data points and zero-filled to 32 K data points before Fourier transformation. For the determination of the amide proton temperature coefficients, 1D spectra were acquired at a 300–340 K temperature range in steps of 5 K. All 2D spectra were recorded in the phase-sensitive mode using time-proportional phase incrementation (TPPI). TOCSY spectra were recorded using the MLEV-17 spin lock sequence [20] with mixing time 80 ms and NOESY spectra with 350 ms mixing time [21]. Two sets of 2D spectra were recorded at 300 and 320 K. Typically, the sweep width was 12 ppm and the spectra were collected into 2048 points in the t_2 dimension (64–136 transients were co-added for each of 400 t_1 points). All NMR spectra were processed using XWIN-NMR version 2.6 and were analyzed on a PC using the Sparky program (T.D. Goddard, D.G. Kneller, SPARKY 3).

Simulated Annealing Calculations

Starting from an extended structure, structural calculations were performed using the simulated annealing and energy minimization protocol in the program CNS, version 1.1 [22]. The procedure included a constant high-temperature (5000 K) torsion-angle annealing protocol, a slow cooling stage with torsion-angle dynamics, and 5000 steps of restraint Powell energy minimization. The resulted structures were sorted in families with common structural characteristics by superimposition using the XCLUSTER 1.2 [23] program, as implemented in the MACROMODEL 6.5 [24] software. XCLUSTER inputs the series of conformations and computes the root mean square (RMS) difference between all possible pairs of conformations. Structures of the input sequence are then reordered on the basis of increasing RMS deviation. Structures were displayed using Maestro 4.1 (Schrödinger Inc., 2001).

RESULTS AND DISCUSSION

In this work, using the alanine scanning methodology, seven peptide analogs corresponding to the α_{IIb} 313–320 sequence were synthesized and tested for their ability to inhibit platelet aggregation. The results from the biological assays have shown that substitution of any particular amino acid within the sequence Y^{313}MES^{316} does not significantly influence the biological activity of the parent peptide (Table 1). However, as it has previously been shown, elimination of the Y^{313}MES^{316} segment and elongation of the *C*-terminal part leads to less active compounds [14]. On the other hand, the R^{317}ADR^{320} sequence seems to be crucial for the expression of the inhibitory activity. Thus, substitution of either R^{317} or D^{319} results in complete abolishment of the activity suggesting that these two amino acids are required for the inhibition of platelet aggregation. The charged side chains of these amino acids and their ability to form a network of hydrogen-bonded and/or ionic interactions could explain their significant contribution to the biological activity. The R^{317} and D^{319} charged side chains are probably involved either in stabilization of the biologically active conformation of the peptide or in a direct interaction with the target molecule (the receptor $\alpha_{IIb}\beta_3$ or fibrinogen). Taking also into account the fact that the mechanism of action of α_{IIb}313–320 differs from that of an RGD peptide [13,] we could attribute this particular biological behavior to the presence of both the Y^{313}MES^{316} segment and the R^{317} and D^{319} amino residues. R^{320} does not seem to substantially influence the biological activity of the analogs; its presence without being indispensable, contributes toward the increase in activity.

DOI: 10.1002/psc

NMR Conformational Analysis

Proton resonances, referenced to the residual DMSO trace, were fully assigned through the combined use of TOCSY and NOESY experiments. The total number of the NOEs was 69 for 8pα_{IIb}314A, 64 for 8pα_{IIb}317A and 83 for 8pα_{IIb}319A. The schematic diagrams of the NOE correlation peaks observed for the three peptides concerning backbone and C^{β} protons are depicted in Figure 1. Sequential NH–NH correlation peaks observed for amino acids spanning peptide sequences from E^{315} to R^{320} imply the formation of loop structures in this region (Figure 1). Interestingly, medium-range correlations were observed in all three peptides especially between the side-chain protons of the charged amino acid residues. Thus, in 8pα_{IIb}314A all E^{315} side-chain protons correlate with R^{317}NH, the R^{317}CH side-chain protons with D^{319}NH and $R^{317}N^{\varepsilon}H$ with $D^{319}C^{\beta}H$. These NOE effects provide a strong evidence for the spatial proximity of R^{317} with both E^{315} and D^{319}. Similar NOE effects were observed between R and D residues in Ac-RGD-NH_2 in DMSO-*d6* solution, which were attributed to the proximity of the side chains due to the presence of an ionic interaction involving the guanidinium and carboxylate groups [25]. In 8pα_{IIb}317A, the E^{315} protons correlate with A^{317}, D^{319} and R^{320}, while in 8pα_{IIb}319A all E^{315} side-chain protons correlate, out of $C^{\alpha}H$, with all the other R^{317} protons suggesting the proximity, and possibly the interaction between the two side chains of these residues.

The low temperature dependence $\Delta\delta/\Delta T$ absolute value observed for the D^{319} backbone amide proton in 8pα_{IIb}314A and 8pα_{IIb}317A indicate that this proton is not entirely exposed to the solvent and is possibly involved in intramolecular interaction. Interestingly, A^{319} amide proton in 8pα_{IIb}319A exhibits a high absolute $\Delta\delta/\Delta T$ value suggesting that the D amino residue in this position plays an important role in the structure stabilization of the parent peptide. The low absolute value $\Delta\delta/\Delta T$ of the *C*-terminal R^{320} amide protons may possibly be derived from the adjacent charged carboxylate groups (Table 2) [26].

In the case of 8pα_{IIb}314A and 8pα_{IIb}319A peptides the $R^{317}N^{\varepsilon}H$ chemical shift was found to be 10.09 and 9.38 ppm, respectively, while in all peptides the $R^{320}N^{\varepsilon}H$ chemical shift was <9 ppm (Table 2). These data imply that $R^{317}N^{\varepsilon}H$ in 8pα_{IIb}314A is involved in a hydrogen bond, while in the case of 8pα_{IIb}319A this bond, if it exists, is much weaker [27–29]. The occurrence of a possible guanidinium–carboxylate interaction between R^{317} and D^{319} in the case of 8pα_{IIb}314A is supported by the behavior of their side chains. Thus, the R^{317} and D^{319} side-chain geminal protons exhibit unusually strong chemical shift differences, probably as a result of their restricted mobility (Table 2). This is clearly evidenced by comparison of R^{317} with R^{320} in the same peptide (8pα_{IIb}314A) or R^{317} in 8pα_{IIb}314A with R^{317} in 8pα_{IIb}319A respectively. The same also holds true

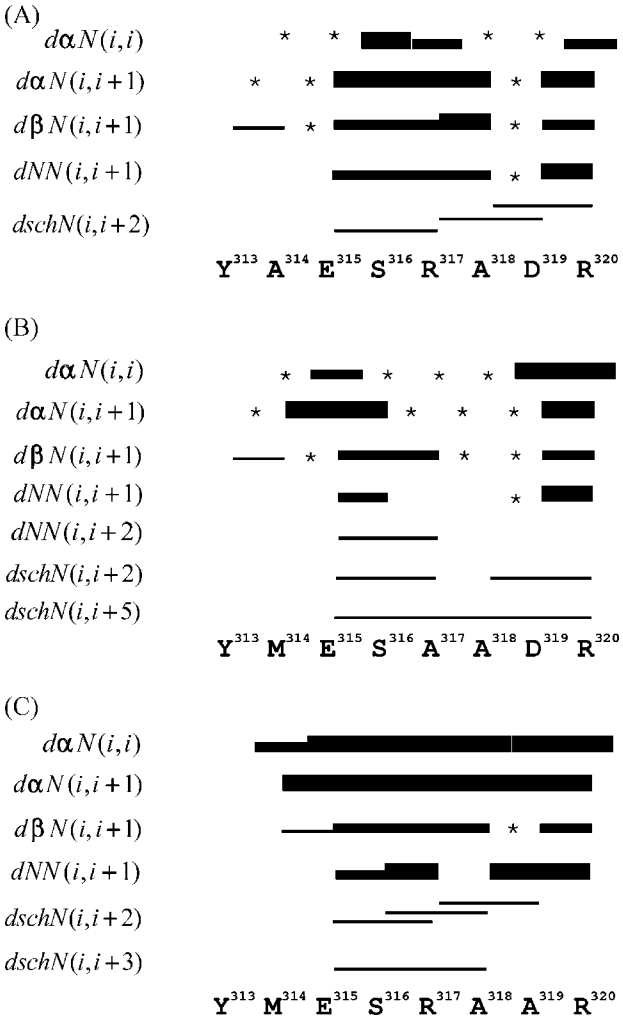

Figure 1 Schematic representation of the observed nOes for the 8pα_{IIb}314A (a), 8pα_{IIb}317A (b) and 8pα_{IIb}319A (c) peptides in DMSO-d_6 solution. Asterisks refer to nOes that cannot be detected or resolved due to severe overlap.

if we compare the D^{319} geminal protons in 8pα_{IIb}314A and 8pα_{IIb}317A respectively (Table 2). In addition, the D^{319} $^3J_{\alpha\beta 1}$ and $^3J_{\alpha\beta 2}$ coupling constant values (4.44 and 4.57 Hz, respectively) in 8pα_{IIb}314A indicate a very high percentage (~61%) of the less energetically favored rotamer g+ ($\chi 1 = 60^{\circ}$). Under these rotational conditions one of the β-COO^- oxygens must be oriented in close proximity to the D^{319} NH proton [25,28,30–32]. This fact can explain the low absolute temperature coefficient observed for the D^{319} NH proton [25].

Comparing the $N^{\eta}{}_2H_4$ NMR signal of R^{320} with the corresponding R^{317} in the 8pα_{IIb}314A peptide spectrum (Figure 2) we observe that the latter still broadens at 320 K and is almost unobservable even at 340 K, while the $R^{320}N^{\eta}{}_2H_4$ signal progressively sharpens suggesting that the $R^{317}N^{\eta}{}_2H_4$ protons exchange slowly, protected probably by the formation of a hydrogen bond. In the case of 8pα_{IIb}319A, the $R^{317}N^{\eta}{}_2H_4$ signal is broader than the corresponding R^{320}, however observable [25,30].

DOI: 10.1002/psc

Table 2 NMR data of of 8pα_{IIb}314A, 8pα_{IIb}317A and 8pα_{IIb}319A peptides in DMSO-d_6 solution

	E^{315}	S	R/A(**$N^{\varepsilon}H$**)	A	D/A	R^{320} (**$N^{\varepsilon}H$**)
NH $\Delta\delta/\Delta T$ (ppb/K)						
8pα_{IIb}314A	−7.6	−5.4	−3.2 (−2.2)	−6.8	−1.9	0.4 (−5.9)
8pα_{IIb}317A	−6.0	−3.1	−2.4	−6.6	−1.1	−0.6 (−6.1)
8pα_{IIb}319A	−7.6	−5.4	−7.0 (−4.9)	−4.1	−5.2	−1.3 (−11.5)
δ $RN^{\varepsilon}H$ (ppm)						
8pα_{IIb}314A	—	—	10.09	—	—	8.58
8pα_{IIb}317A	—	—	—	—	—	8.93
8pα_{IIb}319A	—	—	9.38	—	—	8.16
$\Delta\delta$ $RC^{\gamma}H_2$ (ppm)						
8pα_{IIb}314A	—	—	0.09	—	—	0.00
8pα_{IIb}317A	—	—	—	—	—	—
8pα_{IIb}319A	—	—	0.11	—	—	0.00
$\Delta\delta$ $RC^{\delta}H_2$ (ppm)						
8pα_{IIb}314A	—	—	0.15	—	—	0.00
8pα_{IIb}317A	—	—	—	—	—	—
8pα_{IIb}319A	—	—	0.05	—	—	0.00
$\Delta\delta$ $DC^{\beta}H_2$ (ppm)						
8pα_{IIb}314A	—	—	—	—	0.47	—
8pα_{IIb}317A	—	—	—	—	0.29	—
8pα_{IIb}319A	—	—	—	—	—	—

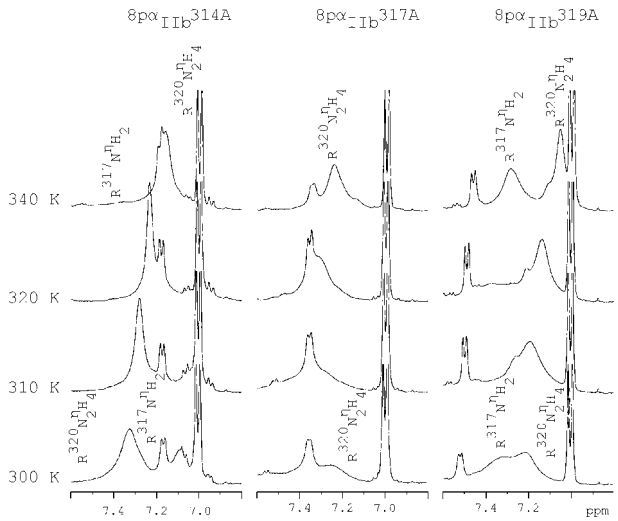

Figure 2 400 MHz ^{1}H NMR spectra showing the behavior of the R $N_2{}^{\eta}H_4$ protons of 8pα_{IIb}314A, 8pα_{IIb}317A and 8pα_{IIb}319A peptides in DMSO-d_6 solution at various temperature values.

The temperature coefficients, the deshielding of $RN^{\varepsilon}H$ at position 317, the broadening behavior of $N^{\eta}{}_2H_4$ comply with an interaction of guanidinium of R^{317}, probably an intramolecular hydrogen bond, in both 8pα_{IIb}314A and 8pα_{IIb}319A peptides, however less intense in the case of 8pα_{IIb}319A [25,30].

Simulated annealing molecular calculations performed by the CNS program using the derived nOe correlations in order to sample the conformational space of the three peptides. The program XCLUSTER 1.2, as implemented in MACROMODEL 6.5 package (Schrödinger Inc.), was used to assemble the generated structures into conformational families based on geometrical similarities. The classification shows that the generated structures diversify mainly by their highly flexible *N* terminus. The representative structures of each different conformational family for the 8pα_{IIb}314A, 8pα_{IIb}317A and 8pα_{IIb}319A peptides can be clustered as shown in Figure 3(a)–(c), respectively. The representative configuration of the most populated family for each peptide is also shown (Figure 3(b), (d), (f)). The mutual RMS deviation of the members of these families is provided in Table 3.

As is shown in Figure 3(a) in the case of 8pα_{IIb}314A peptide the conformations that resulted from the calculations share a lot of similarities, suggesting the existence of a solid and stable structural organization of this sequence. Two nearly 90°-bends localized in S^{316} (phi ~85°) and A^{318} (phi ~80°) vicinity result more or less in the inversion of the backbone orientation. This characteristic conformation is probably dictated by the dual interaction of R^{317} side chain with both E^{315} and D^{319} carboxylate groups that places all three side chains toward the same side of the backbone. The guanidino group of R^{317} seems to form salt bridges with both E^{315} and D^{319}. In addition, this spatial arrangement of the side chains contributes to the weakness of the ionic interaction between R^{317} and D^{319}. These findings are in good agreement with the established conformational criteria for an inhibitor of human platelet aggregation. Both criteria, the synplanar orientation of the R^{317} and

DOI: 10.1002/psc

Table 3 Classification of restraints and structure statistics

Restraint classification	Peptide		
	8pα_{IIb}314A	8pα_{IIb}317A	8pα_{IIb}319A
Total number of NOEs	69	62	83
Number of intraresidue NOEs	31	35	38
Number of interresidue NOEs	38	27	45
Number of strong NOEs (<3.0 Å)	10	11	23
Number of medium NOEs (<3.9 Å)	26	33	41
Number of weak NOEs (<5 Å)	33	18	19
Number of hydrogen bonds	2	0	0
Calculation results			
Number of structures calculated	100		
Number of distance restraint violations >0.3 Å	0	0	1
Number of distance restraint violations >0.2 Å	0	0	3
Number of structures of the most populated family	58	51	43
Average r.m.s.d. (Å) for backbone atoms	0.35 ± 0.17;	0.51 ± 0.26;	0.20 ± 0.14
Aligned on backbone atoms of residues	E^{315}–D^{319}	E^{315}–R^{320}	E^{315}–R^{320}
Average r.m.s.d (Å) for heavy atoms	1.08 ± 0.30;	1.53 ± 0.44;	1.25 ± 0.37
Aligned on backbone atoms of residues	E^{315}–D^{319}	E^{315}–R^{320}	E^{315}–R^{320}

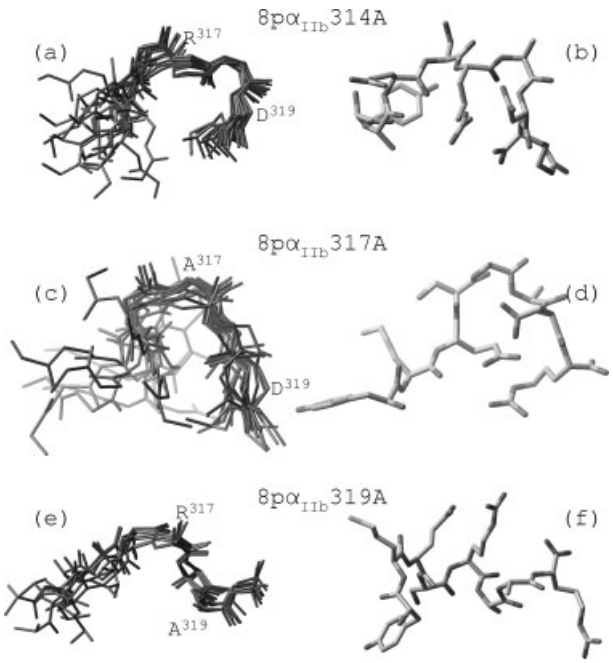

Figure 3 Bundle of representative structures of the different conformational families resulted from the calculations based on experimental data for peptides 8pα_{IIb}314A [(a) superimposed on backbone heavy atoms of residues E^{315}–D^{319}], 8pα_{IIb}317A [(c) superimposed on the E^{315}–R^{320} backbone heavy atoms], and 8pα_{IIb}319A [(e) superimposed on the E^{315}–R^{320} backbone heavy atoms], and the energy-minimized structure of the most populated family [(b), (d) and (e), respectively].

D^{319} side chains and the low strength of their ionic interaction have been evaluated from structure–activity studies of (*S*, *S*)–RCDC – containing analogs [30,33,34]. Interestingly the compounds that satisfy these criteria exhibit a non-RGD-like inhibitory activity on human platelet aggregation [34]. The same also holds true for the α_{IIb}313–320 peptide [13].

In the case of 8pα_{IIb}317A peptide, a more closed turnaround S^{316} and R^{317} is formed, probably stabilized by the week interaction between R^{320} and E^{315} side chains. In the 8pα_{IIb}319A sequence, the interaction between the side chains of R^{317} and E^{315} does not require any special arrangement of the backbone, and as a consequence, an almost extended loop is occupied. The loss of activity in the case of these two derivatives can be attributed either to complete alteration of the bioactive conformation or to the absence of the charged side chain which is required for a direct contact with a complimentary group of the target protein (receptor or fibrinogen).

CONCLUSIONS

The present study attempted to explore the structural and conformational factors that influence the inhibitory activity of the α_{IIb}313–320 sequence of the $\alpha_{IIb}\beta_3$ receptor on the aggregation of human platelets. Using the alanine scanning approach, seven α_{IIb}313–320 peptide analogs were synthesized and tested for their inhibitory activity. The results from the biological assays have shown that substitution of any particular amino acid within the sequence $Y^{313}MES^{316}$ does not significantly influence the biological activity of the parent peptide. On the other hand, the $R^{317}ADR^{320}$

DOI: 10.1002/psc

sequence seems to be crucial for the expression of the inhibitory activity. Thus, substitution of either R^{317} or D^{319} results in complete abolishment of the activity. The charged side chains of these amino acids and their ability to form a network of hydrogen-bonded and/or ionic interactions could explain their significant contribution to the biological activity.

The biological behavior of the α_{IIb}313–320 analogs is in fairly good agreement with the results of the conformational studies that have revealed a specific contribution of R^{317} and D^{319} in the stabilization of conformation. The ^{1}H NMR and simulated annealing molecular calculations studies have shown that the R^{317} and D^{319} side chains in the active 8pα_{IIb}314A are oriented toward the same side of the molecule. The interaction of the R^{317} guanidinium group with both E^{315} the D^{319} carboxylate groups leads to a weakness of R^{317} and D^{319} ionic interaction, which in turn, favors increase in the activity [33]. The loss of activity in the case of 8pα_{IIb}317A and 8pα_{IIb}319A further confirms the significant role of R^{317} and D^{319} amino residues in both the stabilization of the conformation and the activity of the parent α_{IIb}313–320 sequence.

Acknowledgements

We acknowledge GSRT and EU (EPAN YB/88) for their financial support.

REFERENCES

1. Philips DR, Charo IF, Parise LV, Fitzgerald LA. The platelet membrane glycoprotein IIb-IIIa complex. *Blood* 1988; **71**: 831–843.
2. Calvete JJ. Platelet integrin GPIIb/IIIa: structure-function correlations. An update and lessons from other integrins. *Proc. Soc. Exp. Biol. Med.* 1999; **222**: 29–38.
3. Giltay JC, Leeksma OC, Breederveld C, van Mourik JA. Normal synthesis and expression of endothelial IIb/IIIa in Glanzmann's thrombasthenia. *Blood* 1987; **69**: 809–812.
4. Tsikaris V. The anti-platelet approach targeting the fibrinogen ligand of the GPIIb/IIIa receptor. *J. Pept. Sci.* 2004; **10**: 589–602.
5. Biris N, Abatzis M, Mitsios JV, Sakarellos-Daitsiotis M, Sakarellos C, Tsoukatos D, Tselepis AD, Michalis L, Sideris D, Konidou G, Soteriadou K, Tsikaris V. Mapping the binding domains of the α_{IIb} subunit. A study performed on the activated form of the platelet integrin $\alpha_{IIb}\beta_3$. *Eur. J. Biochem.* 2003; **270**: 3760–3767.
6. Ambo H, Kamata T, Handa M, Kawai Y, Oda A, Murata M, Takada Y, Ikeda Y. Novel point mutations in the α_{IIb} subunit (Phe289 Ser, Glu324 → Lys and Gln747 → Pro) causing thrombasthenic phenotypes in four Japanese patients. *Br. J. Haematol.* 1998; **102**: 829–840.
7. Ferrer M, Fernandez-Pinel M, Gonzalez-Manchon C, Gonzalez J, Ayuso MS, Parrilla R. A mutant (Arg327 → His) GPIIb associated to thrombasthenia exerts a dominant negative effect in stably transfected CHO cells. *Thromb. Haemostasis* 1996; **76**: 292–301.
8. Ruan J, Peyruchaud O, Alberio L, Valles G, Clemetson K, Bourre F, Nurden AT. Double heterozygosity of the GPIIb gene in a Swiss patient with Glanzmann's thrombasthenia. *Br. J. Haematol.* 1998; **102**: 918–925.
9. Tao J, Arias-Sagado EG, Gonzalez-Manchon C, Iruin G, Butta N, Ayuso MS, Parrilla R. A 1063G → A mutation in exon 12 of glycoprotein (GP) IIb associated with a thrombasthenic phenotype: mutation analysis of [324E] GPIIb. *Br. J. Haematol.* 2000; **111**: 965–973.
10. Derrick JM, Taylor DB, Loudon RG, Gartner TK. The peptide LSARLAF causes platelet secretion and aggregation by directly activating the integrin α_{IIb} β_3. *Biochem. J.* 1997; **325**: 309–313.
11. Derrick JM, Loudon RG, Gartner TK. Peptide LSARLAF activates $\alpha_{IIb}\rightarrow_3$ on resting platelets and causes resting platelet aggregate formation without platelet shape change. *Thromb. Res.* 1998; **89**: 31–40.
12. Derrick JM, Shattil SJ, Poncz M, Gruppo RA, Gartner TK. Distinct domains of α_{IIb} β_3 support different aspects of outside-in signal transduction and platelet activation induced by LSARLAF, an α_{IIb} β_3 interacting peptide. *Thromb. Haemostasis* 2001; **86**: 894–901.
13. Mitsios JV, Tambaki AP, Abatzis M, Biris N, Sakarellos-Daitsiotis M, Sakarellos C, Soteriadou K, Goudevenos J, Elisaf M, Tsoukatos D, Tsikaris V, Tselepis AD. Effect of synthetic peptides corresponding to residues 313–332 of α_{IIb} subunit on platelet activation and fibrinogen binding to $\alpha_{IIb}\beta_3$. *Eur. J. Biochem.* 2004; **271**: 855–862.
14. Mitsios JV, Stamos G, Rodis FI, Tsironis LD, Stanica M-R, Sakarellos C, Tsoukatos D, Tsikaris V, Tselepis AD. Investigation of the role of adjacent amino acids to the 313–320 sequence of the α_{IIb} subunit on platelet activation and fibrinogen binding to $\alpha_{IIb}\beta_3$. *Platelets* 2006; **17**: 277–282.
15. Jones J. Abbreviations and symbols in peptide science: a revised guide and commentary. *J. Pept. Sci.* 2006; **12**: 1–12.
16. Stewart JM, Young JD. *Solid Phase Peptide Synthesis*. Pierce Chem. Co.: Rockford, IL, 1984; 71–95.
17. Atherton E, Sheppard RC. *Solid Phase Peptide Synthesis: A Practical Approach*. IRL Press: Oxford, 1989.
18. Bodansky M, Bodansky A. *The Practice of Peptide Synthesis*, 2nd edn. Springer: Berlin, 1994.
19. Tsikaris V, Cung MT, Panou-Pomonis E, Sakarellos C, Sakarellos-Daitsiotis M. ^{1}H NMR studies on the preferred interactions of guanidinium and C-terminal carboxylate groups in arginine containing peptides. *J. Chem. Soc., Perkin Trans. 2* 1993; 1345–1349.
20. Bax A, Davis DG. MLEV-17-based two-dimensional homonuclear magnetization transfer spectroscopy. *J. Magn. Reson.* 1985; **65**: 355–360.
21. Kumar A, Ernst RR, Wüthrich K. A two-dimensional nuclear Overhauser enhancement (2D NOE) experiment for the elucidation of complete proton-proton cross-relaxation networks in biological macromolecules. *Biochem. Biophys. Res. Commun.* 1980; **95**: 1–6.
22. Brunger AT, Adams PD, Clore GM, DeLano WL, Gros P, Grosse-Kunstleve RW, Jiang JS, Kuszewski J, Nilges M, Pannu NS, Read RJ, Rice LM, Simonson T, Warren GL. Crystallography and NMR system. A new software suite for macromolecular structure determination. *Acta Crystallogr., Sect. D* 1998; **54**: 905–921.
23. Shenkin PS, McDonald DQ. Cluster-analysis of molecular conformations. *J. Comput. Chem.* 1994; **15**: 899–916.
24. Mohamadi F, Richards NGJ, Guida WC, Liskamp R, Lipton M, Caufield C, Chang G, Hendrickson T, Still WC. MACROMODEL. An integrated software system for modeling organic and bioorganic molecules using molecular mechanics. *J. Comput. Chem.* 1990; **11**: 440–467.
25. Biris N, Stavrakoudis A, Politou AS, Mikros E, Sakarellos-Daitsiotis M, Sakarellos C, Tsikaris V. The Ac-RGD-NH_2 peptide as a probe of slow conformational exchange of short linear peptides in DMSO. *Biopolymers* 2003; **69**: 72–86.
26. Tsikaris V, Sakarellos C, Sakarellos-Daitsiotis M, Orlewski P, Marraud M, Cung MT, Vatzaki E, Tzartos S. Construction and application of a new class of sequential oligopeptide carriers (SOC_n) for multiple anchoring of antigenic peptides: application to the acetylcholine receptor (AChR) main immunogenic region. *Int. J. Biol. Macromol.* 1996; **19**: 195–205.
27. Tsikaris V, Sakarellos-Daitsiotis M, Panou-Pomonis E, Detsikas E, Sakarellos C, Cung MT, Marraud M. ^{1}H NMR studies on arginine

tripeptides: evidence for guanidinium-C-terminal carboxylate interactions. *Pept. Res.* 1992; **5**: 110–114.

28. Tsikaris V, Sakarellos-Daitsiotis M, Tzovaras D, Sakarellos C, Orlewski P, Cung MT, Marraud M. Isomerization of the Xaa-Pro peptide bond induced by ionic interactions of arginine. *Biopolymers* 1996; **38**: 673–682.
29. Tsikaris V, Cung MT, Sakarellos C, Tzinia AK, Soteriadou KP, Sakarellos-Daitsiotis M. NMR study on a SRYD-containing fibronectin-like sequence (250–257) of Leismania gp63: Contribution of residual water in the dimethyl sulfoxide solution structure. *J. Chem. Soc., Perkin Trans. 2* 1994; 821–826.
30. Kostidis S, Stavrakoudis A, Biris N, Tsoukatos D, Sakarellos C, Tsikaris V. The relative orientation of the Arg and Asp side chains defined by a pseudodihedral angle as a key criterion for evaluating the structure-activity relationship of RGD peptides. *J. Pept. Sci.* 2004; **8**: 494–509.
31. Benedetti E, Morelli G, Némethy G, Scheraga HA. Statistical and energetic analysis of side-chain conformations in oligopeptides. *Int. J. Pept. Protein Res.* 1983; **22**: 1–15.
32. McGregor MJ, Islam SA, Sternberg MJ. Analysis of the relationship between side-chain conformation and secondary structure in globular proteins. *J. Mol. Biol.* 1987; **198**: 295–310.
33. Stavrakoudis A, Bizos G, Eleftheriadis D, Kouki A, Panou-Pomonis E, Sakarellos-Daitsiotis M, Sakarellos C, Tsoukatos D, Tsikaris V. A three-residue cyclic scaffold of non-RGD containing peptide analogues as platelet aggregation inhibitors: design, synthesis, and structure-function relationships. *Biopolymers* 2001; **56**: 20–26.
34. Kouki A, Mitsios JV, Sakarellos-Daitsiotis M, Sakarellos C, Tselepis AD, Tsikaris V, Tsoukatos DC. Highly constrained cyclic (S,S)-CXaaC-peptides as inhibitors of fibrinogen binding to platelets. *J. Thromb. Haemostasis* 2005; **3**: 2324–2330.

DOI: 10.1002/psc